

JOURNAL OF TECHNIQUES

Journal homepage: http://journal.mtu.edu.iq



REVIEW ARTICLE – MATERIAL SCIENCE (MISCELLANEOUS)

Research Progress on Growth Mechanisms of Helical Carbon Nanofibers

Xialong Cai¹, Rongling Zhang¹, Wei Feng¹, Hanjun Wei², Ying Li^{1*}, Mazin S. Ibrahim³, Shrouq Z. Almaaitah⁴

¹School of Mechanical Engineering, Chengdu University, 2025 Chengluo Avenue, Chengdu 610106, China ²Institute for Advanced Study, Chengdu University, 2025 Chengluo Avenue, Chengdu 610106, China

³Green Electronics Oxide nanomaterials Group (GEM), School of Materials and Mineral Resources Engineering, Engineering Campus, Universiti Sains Malaysia, 14300 Nibong Tebal, Pulau Pinang, Malaysia

⁴School of Civil Engineering-Structural Engineering, Engineering Campus, Universiti Sains Malaysia, 14300 Nibong Tebal, Pulau Pinang, Malaysia

* Corresponding author E-mail: liying@cdu.edu.cn

Article Info.	Abstract
Article history:	Helical carbon nanofibers (HCNFs), a novel class of nanocarbon materials with a unique three-dimensional helical morphology, inherit many of the intrinsic properties of conventional carbon nanofibers while exhibiting additional
Received 31 July 2025	characteristics such as superelasticity, unique electromagnetic response behavior, and a highly textured surface topology. These properties make HCNFs highly valuable for applications in electromagnetic shielding, nanosprings, and sensing technologies. Among the various fabrication techniques, chemical vapor deposition remains the most widely used and
Accepted 12 September 2025	effective method for producing HCNFs, with structural regulation achieved by controlling parameters such as catalyst type and reaction temperature. Alternative methods such as flame synthesis, electrospinning, and templating have also demonstrated potential in growing HCNFs. Regarding growth mechanisms, the asymmetric carbon deposition and
Publishing 30 September 2025	diffusion on catalyst surfaces are considered the primary drivers of the periodic curling behavior observed in HCNFs Several models, including the three-dimensional growth mechanism, the vapor-liquid-solid-solid mechanism, and the coordination polymerization mechanism, have been proposed to elucidate the formation of helical structures. This review provides a comprehensive overview of recent advancements in HCNF growth mechanisms, emphasizing the roles of precursor materials, catalyst properties, and reaction conditions in achieving precise and controllable synthesis.

Keywords: Helical Carbon Nanofibers (HCNFs); Fabrication Methods; Growth Mechanisms.

1. Introduction

Helical carbon nanofibers (HCNFs) are a distinctive form of carbon nanostructure characterized by a unique three-dimensional coiled geometry. Since their initial observation in 1953 during the catalytic decomposition of carbon monoxide, these nanomaterials have attracted considerable research attention due to their spatial complexity, outstanding physicochemical properties, and broad application prospects [1]. With advances in nanotechnology, diverse morphologies of HCNFs have been synthesized, including kinked-twisted [2], single-helical [3], double-helical [4], flattened [5], and carbon nanotubes (CNTs) with embedded helical segments [6]. Carbon nanofibers (CNFs) are known for their low density, high tensile strength, excellent thermal conductivity, and electromagnetic shielding capabilities, with anisotropic mechanical, thermal, and electrical properties [7, 8]. HCNFs retain most of these attributes while gaining additional features from their helical structure. Mechanically, the coiled structure imparts superelasticity and reversible extensibility [9]. Physically, it enables distinct electromagnetic interactions, such as enhanced wave scattering and absorption. Structurally, the three-dimensional morphology increases the specific surface area and exposes abundant topological features, providing more active sites for molecular adsorption and functionalization [10, 11]. As a result, HCNFs have demonstrated promising applications in electromagnetic shielding, nanoactuators, flexible electronics, and biomedicine [12]. Recent studies have explored their use in electrochemical sensing [13], as reinforcing fillers in rubber composites [14], in electromagnetic wave absorption [15], and as conductive frameworks for lithium-ion battery electrodes [16]. Despite these advances, the growth mechanism of HCNFs remains a topic of ongoing investigation. Understanding their formation involves multiscale and multidisciplinary challenges, including catalyst evolution, gas adsorption and decomposition, atomic diffusion, and helical nucleation dynamics. This review aims to comprehensively summarize recent progress on the growth mechanisms of HCNFs, with an emphasis on the role of catalyst properties, carbon precursors, and reaction parameters in controlling their structure.

Nomenclature & Symbols					
HCNFs	Helical Carbon Nanofibers	CNTs	Carbon Nanotubes		
CVD	Chemical Vapor Deposition	VLS	Vapor-Solid-Liquid		
VLSS	Vapor-Liquid-Solid-Solid	DFT	Density Functional Theory		

2. Typical Preparation Methods of HCNFs

2.1. Chemical Vapor Deposition (CVD)

Chemical vapor deposition (CVD) is the most commonly adopted and effective technique for the synthesis of HCNFs. By regulating factors such as catalyst composition, morphology, particle size, carbon source, reaction temperature, gas flow rate, and growth time, researchers can tailor the resulting fiber morphology and helical characteristics. The CVD growth process typically involves three stages: (1) decomposition of the carbon source, (2) diffusion of carbon atoms, and (3) nucleation and precipitation into fiber structures [17].

As early as 2004, Qin et al. [18] reported the formation of symmetrically grown HCNFs using copper tartrate as a catalyst precursor, and attributed the fiber morphology to the shape evolution of Cu nanoparticles. Tang et al. [19] synthesized symmetric double-helical CNFs using Fe nanoparticles, observing nearly identical coil parameters (diameter, pitch, length) but opposite chirality (Fig. 1). Their structural analysis revealed a (110) crystal plane as the symmetry center, suggesting that differential deposition on specific crystal facets drives helical growth. Yu et al. [20] extended this approach using Cu-Ni alloy nanoparticles synthesized via hydrogen arc plasma. The polyhedral catalyst morphology facilitated dual active sites, promoting symmetric carbon diffusion and resulting in HCNFs with matching periodicity but opposite chirality. Their findings also indicated that surface reconstruction of alloy catalysts at low temperature plays a crucial role in symmetric helical growth.

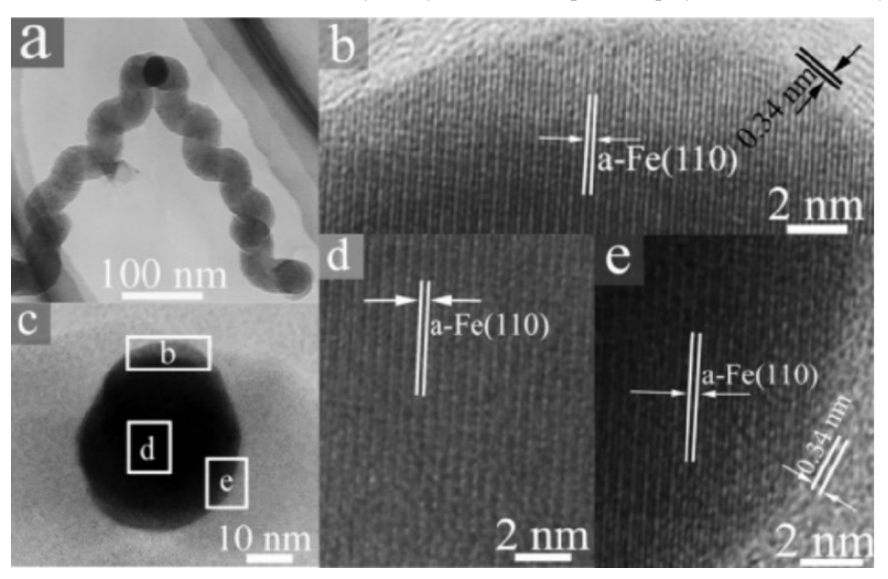


Fig. 1. Microstructure of a catalyst nanoparticle located at the node of coiled nanofibers; (a) TEM image, (b, d, and e) magnified images of areas marked in Fig. (c), respectively, (c) HRTEM image, Copyright 2025 Elsevier Ltd. [19]

As shown in Fig. 2a, the study [21] reported research on the successful growth of helical carbon nanofibers (HCNFs) on a Cu-foil substrate at 980 °C, using ethanol as the carbon precursor. The key mechanism involves the thermal decomposition of ethanol into ethylene and water. The generated water acts as an etchant, removing amorphous carbon that accumulates on the surface of Cu nanoparticles (Cu-NPs), thereby preserving their catalytic activity. At elevated temperatures, Cu-NPs adopt irregular morphologies with sharp edges and corners, which induce uneven carbon precipitation rates across different surface regions. Additionally, the inherently low surface energy of copper inhibits random stacking of carbon layers and facilitates the orderly growth of helical structures. In a related study, Cui et al. [22] grew HCNTs by using Fe₃O₄ nanoparticles, which were reduced to Fe active sites via hydrogen reduction at 425°C. Priscillal et al. [23] investigated that the growth of HCNTs is driven by the synergistic effect of carbon source deposition, catalyst morphology, and catalytic properties. At 600°C, when the carbon source generated from acetylene decomposition diffuses on the surface of the LaNi₅Pt_{0.5} catalyst, pentagon-heptagon structures are easily introduced into the graphite framework due to the low diffusion rate, inducing molecular strain. Meanwhile, the sharp edges of catalyst particles result in an irregular surface, leading to uneven carbon precipitation rates at different positions. Additionally, there is a strong catalytic anisotropy in carbon deposition on different crystal planes of the catalyst. These three factors together promote the coiling of carbon tubes to form a helical structure, with the morphology shown in Fig. 2c. Fig. 2 (f-h) systematically explains the mechanism of how changes in catalyst morphology induced by different reaction temperatures affect the growth of CNTs and the causes of morphological differences.

Radnia et al. [24] proposed that the morphology of CNFs is regulated by the interaction between metal loading and reaction temperature, which macroscopically provides a new parameter dimension for the regulation of helical structures. Jin et al. [25] pointed out that different synthesis temperatures affect the nucleation modes of Cu-based catalysts, which ultimately influence the content and morphology of HCNFs. As shown in Fig. 3(a-d), Jian et al. [26] found that when Cu nanoparticles agglomerate, they cannot expose sufficient crystal planes, making it difficult to induce helical growth. In contrast, uniformly dispersed Cu particles expose more active crystal planes, ultimately generating high-purity HCNFs. Meanwhile, Fig. 3e reveals that the interaction between the gas-induced effect, thermal effect, and size effect regulates the size of Cu nanoparticles, causing the morphology of CNFs to gradually transform from curved fibers to helical fibers and then to straight fibers as the size of the nanoparticles increases.

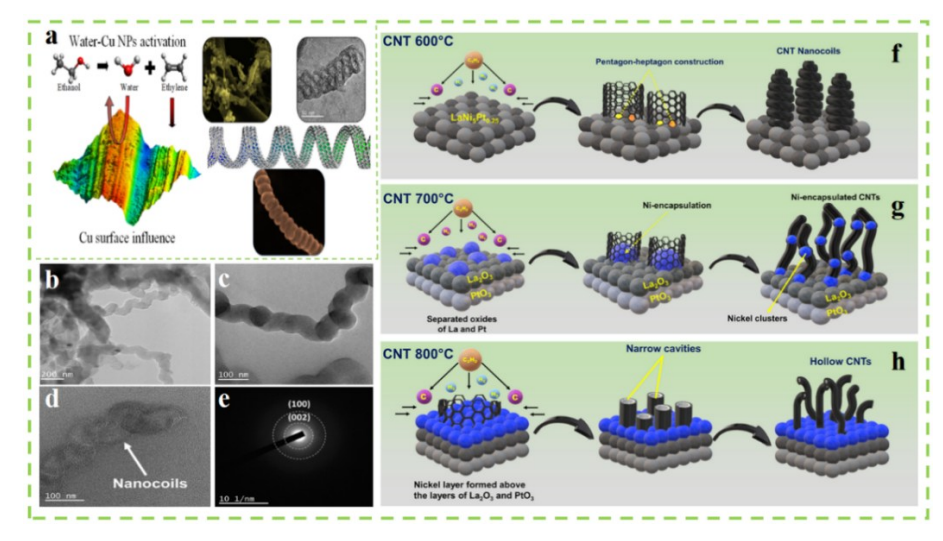


Fig. 2. (a) Experimental Mechanism Diagram, Copyright 2019 Elsevier Ltd. [21], (b-d) TEM micrographs, (e) SAED pattern, (f-h) Schematic illustration of growth mechanism for the CNTs grown at different reaction temperatures from 600°C to 800°C, Copyright 2023 Elsevier B.V. [23]

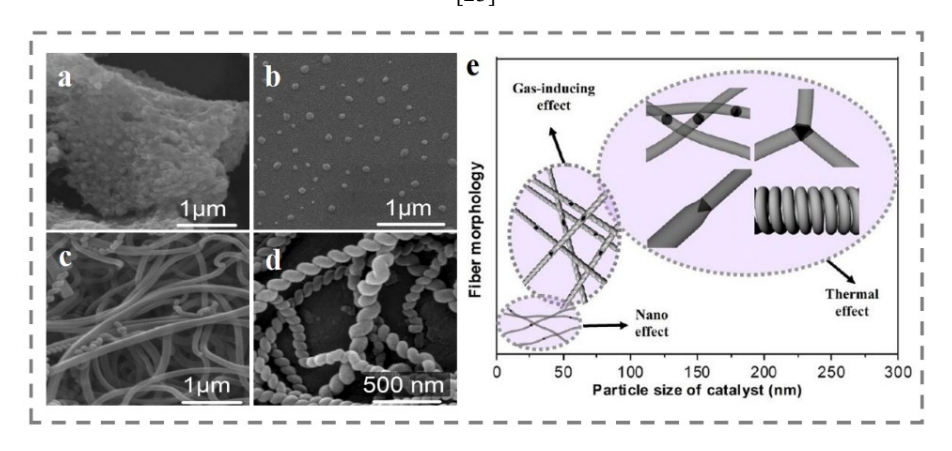


Fig. 3. Catalyst particles; (a, b) and their morphologies, (c, d) of two different types of carbon fibers, (e) Interplay among gas-inducing, thermal, and size effects on the formation of carbon fibers, Copyright 2012 American Chemical Society [26]

Suda et al. [27] used the spin-coating method to reduce the particle size of Fe₂O₃ to the nanoscale, thereby inhibiting the formation of non-helical carbon layers. They also proposed the effects of two catalyst structure growth models on the growth of HCNFs. As shown in Fig. 4, in the Fe₂O₃/SnO₂ model, C₂H₂ directly contacts Fe₂O₃. Fe₂O₃ forms nanoparticles to absorb carbon atoms, and part of C₂H₂ reduces SnO₂ to generate liquid Sn, which diffuses to form Fe-Sn alloys. HCNFs grow on these alloys; however, since Fe₂O₃ directly contacts the carbon source, Fe in it provides strong carbon segregation ability, leading to the formation of a relatively thick carbon layer without a helical structure. As a result, the purity of HCNFs is only 69%±2%. In the SnO₂/Fe₂O₃/SnO₂ model, the upper SnO₂ limits the amount of C₂H₂ reaching the intermediate Fe₂O₃. After Fe₂O₃ absorbs carbon, Fe-Sn alloys are formed on its upper and lower surfaces, and HCNFs grow from these alloys. Due to the regulated supply of carbon sources, the carbon layer without a helical structure becomes thinner, and more carbon is used for the growth of HCNFs, thus increasing the purity of HCNFs to 81%±2%.

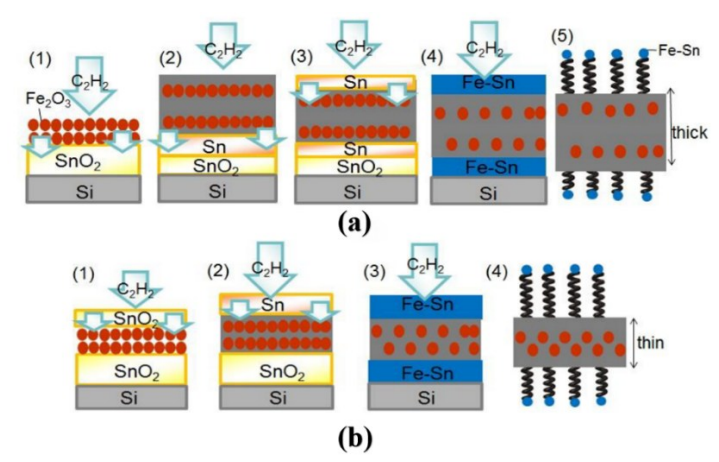


Fig. 4. Growth models of (a) Fe₂O₃/SnO₂, and (b) SnO₂/Fe₂O₃/SnO₂ catalyst structures [27]

In a recent study, Li et al. [28] used the CVD method, with acetylene as the carbon source and copper nanoparticles as the catalyst, to achieve the controllable preparation of kinked and spring-like helical carbon nanofibers by regulating the synthesis temperature and heating rate, as shown in Fig. 5a. They found that when the temperature was uniformly raised to 280°C at a slow heating rate of 1°C/min, the copper nanoparticles maintained a small and uniform size. At this time, the asymmetric deposition of the carbon source on the catalyst surface and the defect-induced effect promoted the twisted growth of the fibers, forming kinked helical carbon nanofibers. When the heating temperature was increased to 380°C, the carbon diffusion rate of copper particles increased, and the periodic deposition behavior of carbon on their surface dominated fiber growth, resulting in spring-like helical carbon nanofibers with a helix size of 40–380 nm and a diameter of 1.75–2.9 μm. Under a fast-heating rate, copper particles were prone to agglomeration, and only CNFs could be grown, with their morphology shown in Fig. 5(b-d). The above results indicate that a slow heating rate is a fundamental prerequisite for the formation of helical structures, while the heating temperature further determines the specific morphology of the helix through carbon deposition.

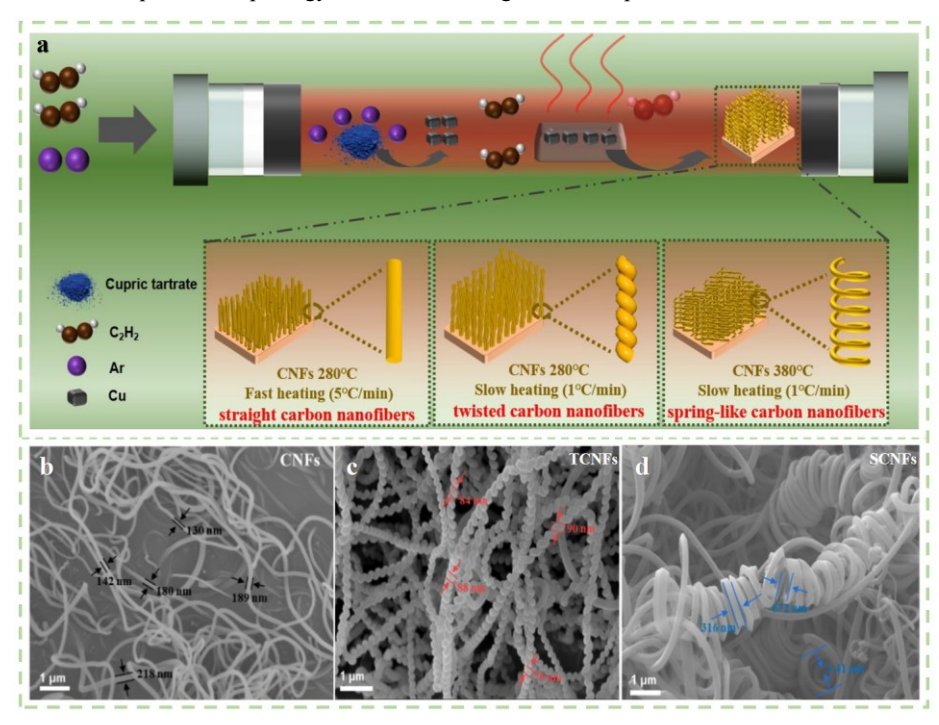


Fig. 5. (a) The synthesis process diagram of CNFs, TCNFs and SCNFs, (b-d) The SEM images of CNFs, TCNFs and SCNFs, Copyright 2024 Elsevier Ltd. [28]

2.2. Other preparation methods

Besides CVD, researchers have also successfully prepared HCNFs using the flame method, spinning method, and template method. In the flame method, Xiong et al. [29] can control the size and morphology of the generated nanoparticles or nanofibers by precisely adjusting parameters such as flame temperature, gas flow rate, and reactant concentration. Zhang et al. [30] demonstrated that Sn-MOF converts into a stable catalytic phase of SnO₂ in an ethanol flame. Subsequently, carbon species undergo adsorption, diffusion, and deposition on its surface via the carbon source in the flame and the organic ligands of Sn-MOF itself. Due to the crystal plane anisotropy of SnO₂, periodic offsets occur during carbon chain growth, leading to the formation of helical structures. Moreover, residual SnO₂ can still generate HCNFs, which confirms its sustained catalytic ability. Meanwhile, prolonging the combustion time increases the length and diameter of HCNFs and makes the helical structure more compact. The preparation process is shown in Fig. 6.

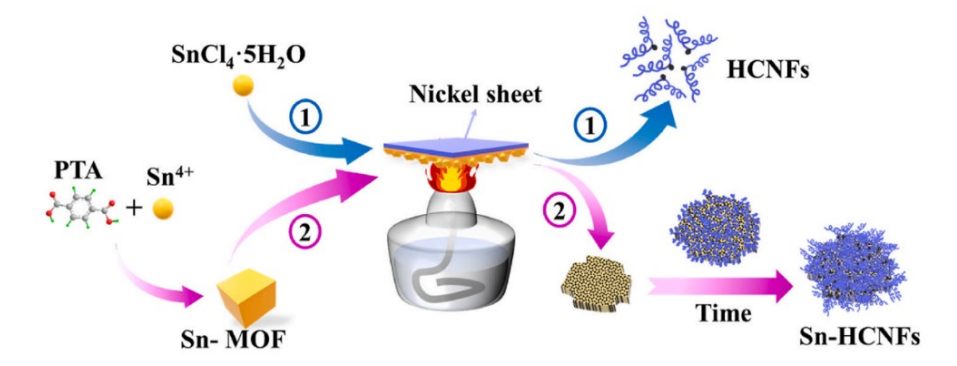


Fig. 6. Schematic illustration of the formation processes of HCNFs (route 1) and Sn-HCNFs (route 2), Copyright 2021 Elsevier B.V. [30]

Electrospun HCNFs have attracted much attention due to their flexibility and ease of fabrication. Dutta et al. [31] used a mixed solution of PAN and nickel acetate as the spinning precursor to prepare CNFs via the electrospinning method. After subsequent stabilization treatment in air at

280°C and carbonization in an inert gas at 700°C, PAN was converted into CNFs, and nickel acetate was synchronously decomposed into Ni nanoparticles, which were anchored on the surface of CNFs. Then, acetylene was introduced at 750°C. The steric hindrance effect caused by the non-streamlined morphology of Ni nanoparticles and the defect-induced curvature from pentagonal/heptagonal carbon ring defects during carbon deposition acted together, leading to the formation of helical structures in CNFs. The supra-templating method, relying on the chiral directional transfer ability of supramolecular templates, can precisely prepare HCNFs with single chirality and high purity, and exhibits unique advantages in terms of structural controllability [32]. Zeli et al. [33] enabled chiral low-molecular-weight gelators to self-assemble into single-chiral helical supramolecular templates through hydrophobic association, hydrogen bonding, and stacking interactions of carbonyl π - π bonds. 1,4-phenylene-bridged silsesquioxane undergoes hydrolysis and condensation under acidic conditions, and directionally deposits on the surface of the template to replicate the helical morphology. After extracting and removing the template, helical polysilsesquioxane fibers are obtained. These fibers form carbon/silicon composite helical fibers after carbonization at 700°C. Finally, SiO₂ is removed while retaining the carbon skeleton to form single-chiral HCNFs, with the helical direction determined and transferred by the chirality of the template.

Other scholars have used naturally occurring helical structures in nature as biological templates, opening up a new path for the large-scale and reproducible preparation of HCNFs [34]. Fig. 7a shows high-purity spiral vessels (SVs) in waste tea leaves. Wang et al. [35] retained their natural helical morphology after carbonization at 500°C to form SV-CFs (HCNFs). A large number of 1–3 nm micropores were generated in the carbon skeleton via KOH etching, resulting in porous SV-ACFs (HCNFs). The helical structure is still determined by the helical morphology of the original template and is stably transferred through the carbonization and pore-forming processes, with the morphology shown in Fig. 7(b-d).

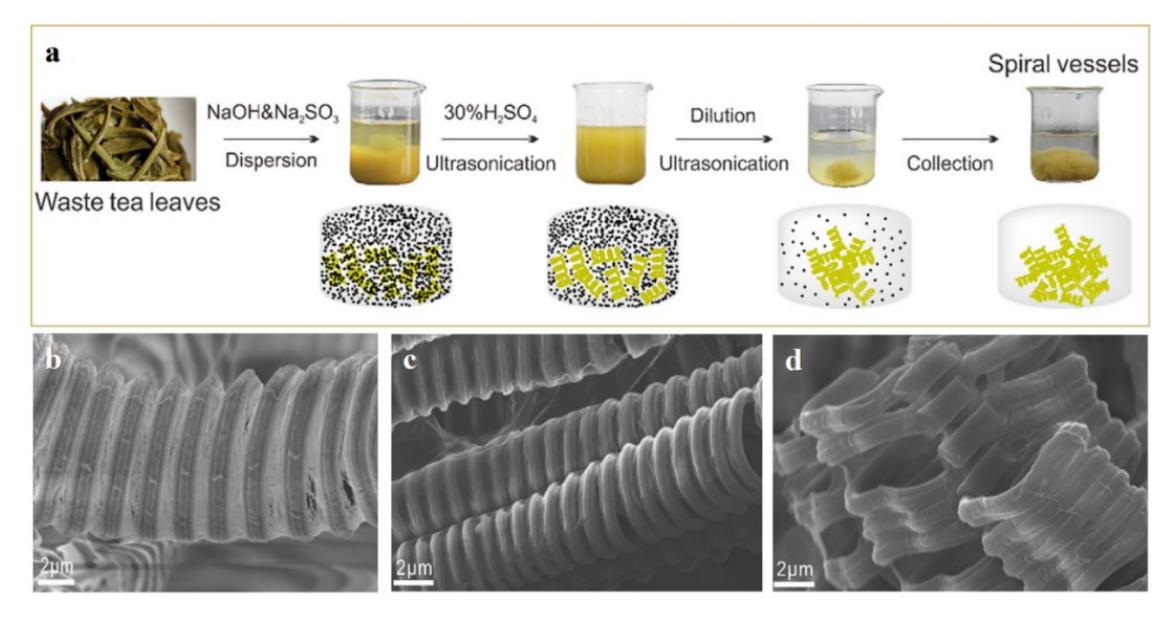


Fig. 7. (a) Schematic extraction of SVs, (b-d) SEM images of SVs, SV-CFs (HCNFs) and SV-ACFs (HCNFs), Copyright 2020 Elsevier Inc. [35]

3. Growth Mechanism of HCNFs

The formation of the above-mentioned helical morphology is attributed to structural regulatory factors such as the anisotropy of each crystal plane of the catalyst and the structural induction of supramolecular or biological templates. Regarding their specific growth mechanisms and growth dynamic mechanisms, scholars have proposed various explanatory models based on different experimental phenomena. It is worth noting that all mechanisms take carbon deposition/diffusion rate differences as the core, and the scope of application of each model essentially reflects the constraint on "whether the rate differences can be stably maintained; deviation from any condition may lead to the failure of the helical structure. Initially, researchers proposed the "vapor-solid-liquid (VLS) growth mechanism" to explain the growth of regularly curled carbon fibers. However, it is difficult to account for the differences in catalytic activity and growth rates among different crystal planes, nor can it explain the formation of other carbon fibers with special shapes [36-38]. As shown in Fig. 8a, based on the 8 fiber loops existing at the growth initiation end of the prepared double-helical carbon fibers and combined with the "VLS mechanism", Chen et al. [39-41] proposed a "threedimensional growth mechanism system" to describe the growth mode of double-helical carbon fibers. In Fig. 8b, it is assumed that six carbon fibers first grow from the six crystal planes of Ni catalytic grains, and then A, B, and C fuse with A', B', and C', respectively, to form two carbon fibers. Due to the anisotropy of carbon deposition on different crystal planes of the grains, the catalytic activity is assumed in the study to follow the order A>B>C. Finally, the two fibers will curl into a helical structure due to the difference in growth rates, as shown in Fig. 8c. This mechanism can effectively explain the growth phenomenon of helical structures and has guiding significance for the controllable preparation of HCNFs helical structures. With the deepening of research, Chen et al. [42] argued that the three-dimensional growth mechanism cannot explain how carbon atoms enter catalyst particles, and the original solid-phase catalytic mechanism also fails to account for the role of thiophene in the synthesis of carbon microcoils. Based on their research, they proposed the vapor-liquid-solid-solid (VLSS) growth mechanism, which can explain the influence of sulfur content in the catalyst on the helical structure.

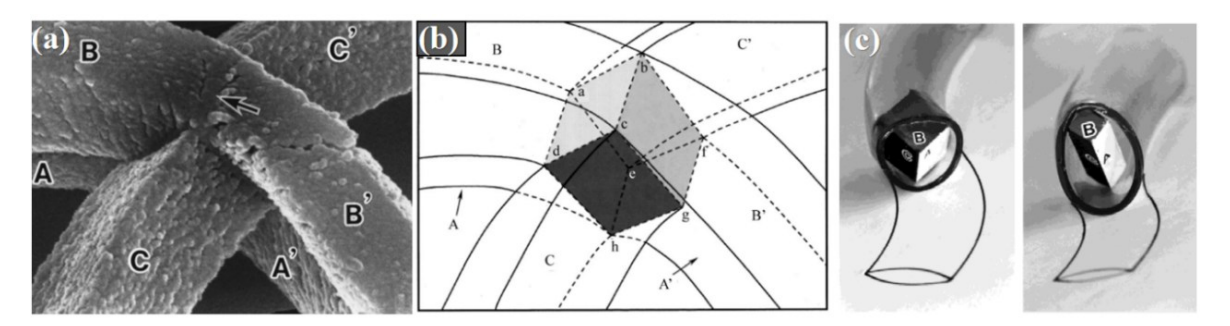


Fig. 8. (a) An enlarged view (arrow indicates a Ni catalyst grain), (b) Postulated Ni catalyst grain (a–h) Cubic-shaped Ni grain embedded in the node of six fibers, (c) Schematic image of growth mechanism of the carbon fibers, Copyright 2002 Elsevier Science B.V. [39-41]

Differences in carbon deposition and diffusion rates on the catalyst are the core driving force for the formation of helical structures. Coville et al. [43], from the perspective of carbon sources, found that unsaturated hydrocarbons are the preferred carbon sources for the efficient growth of helical structures. They easily decompose to produce highly active intermediates containing sp²/sp hybridized carbon, which enhances the difference in carbon deposition rates on the catalyst surface and provides a material basis for the formation of helical structures. Nitze et al. [44], from the perspective of kinetics and catalyst properties, achieved the controllable growth from HCNFs to CNFs by utilizing the "coupling effect of diffusion rate and geometric constraint", and found that their high periodicity is directly related to the morphology of catalyst particles and carbon diffusion kinetics. TEM images in Fig. 9(a-d) show that at 550°C, Pd catalyst particles are triangular or hemispherical with rounded edges, and only contact the fibers on one side. Combined with the growth model in Fig. 9e, partial carbon diffusion paths on their surface are locally blocked, resulting in differences in carbon diffusion rates on both sides of the particles. Moreover, the bidirectional growth characteristic of carbon precipitating symmetrically from both sides of Pd particles causes the fibers to curl periodically, eventually forming HCNFs with uniform pitch and diameter. During the growth process, water can remove obstructions on the catalyst surface through oxidation to regulate the opening of diffusion paths. As the temperature increases, the catalyst particles gradually evolve into symmetric biconical shapes corresponding to straight fibers in the Fig. 9. This transformation can be clearly observed in Fig. 9(f-g): HCNFs transform into straight fibers within dozens of nanometers, and the catalyst particles at the transformation point in the Fig. 9 have begun to evolve into a symmetric morphology, ultimately leading to the transf

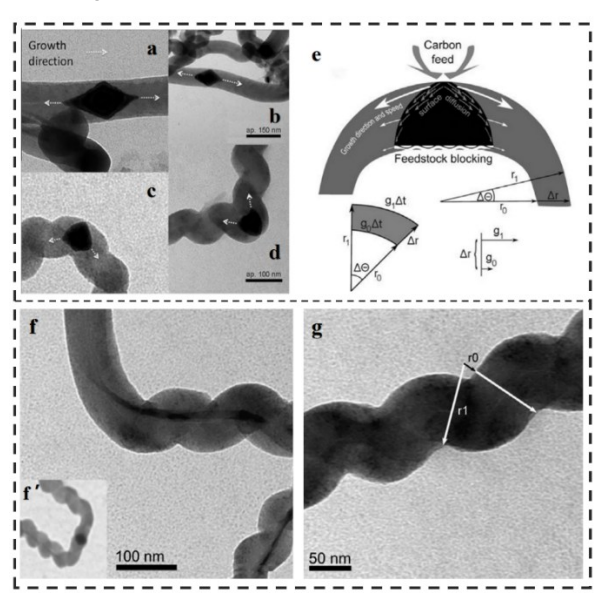


Fig. 9. TEM of catalyst morphologies: rhombic for hollow CNFs; (a, b) edged-hemispherical for helical CNFs, (c, d) (scale bars: averages, shape> size), (e) 2D growth model schematic: go/g1 (inhomogeneous growth), ro/r1 (coil radii), three fibers in different growth states, (f) Helical-to-straight transition bend, (f') Post-transition fiber bend & catalyst morphology (digitally zoomed, showing symmetry), (g) Near-perfect periodicity, ro/r1 as inner/outer coil radii, Copyright 2010 Elsevier Ltd. [44]

The above mechanism is a pure carbon growth process based on differences in carbon deposition or diffusion at medium and high temperatures. Building on this, Jian et al. [45] proposed a coordination polymerization growth mechanism and verified its rationality through experiments and density functional theory (DFT). The researchers prepared HCNFs at low temperatures using copper tartrate as the catalyst precursor. As shown in Fig. 10a, during the coordination polymerization process, the unoccupied 3d and 4f orbitals of Cu nanoparticles first form coordinate bonds with the π electrons of acetylene. After electron rearrangement, these coordinate bonds are converted into covalent bonds, and at the same time, Cu nanoparticles regenerate empty orbitals to adsorb new acetylene molecules, thereby achieving continuous adsorption, activation, and polymerization of acetylene molecules. Meanwhile, the selective adsorption of acetylene on Cu crystal planes, as shown in Fig. 10b, triggers the reconstruction of the catalyst from a quasi-spherical shape to a polyhedral shape, and the proportion of (100) and (111) crystal planes decrease during the reconstruction process. The density functional theory calculation results related to Fig. 11b show that there are differences in the adsorption energy of acetylene on Cu crystal planes, with (110) > (111) > (110). This difference in adsorption energy makes the polymerization rate of acetylene on (100) and (111) crystal planes significantly higher than that on the (110) crystal plane. The difference in

coordination polymerization rates among different Cu crystal planes forces the fibers to extend along a kinked path, thereby forming a symmetric double-helical structure.

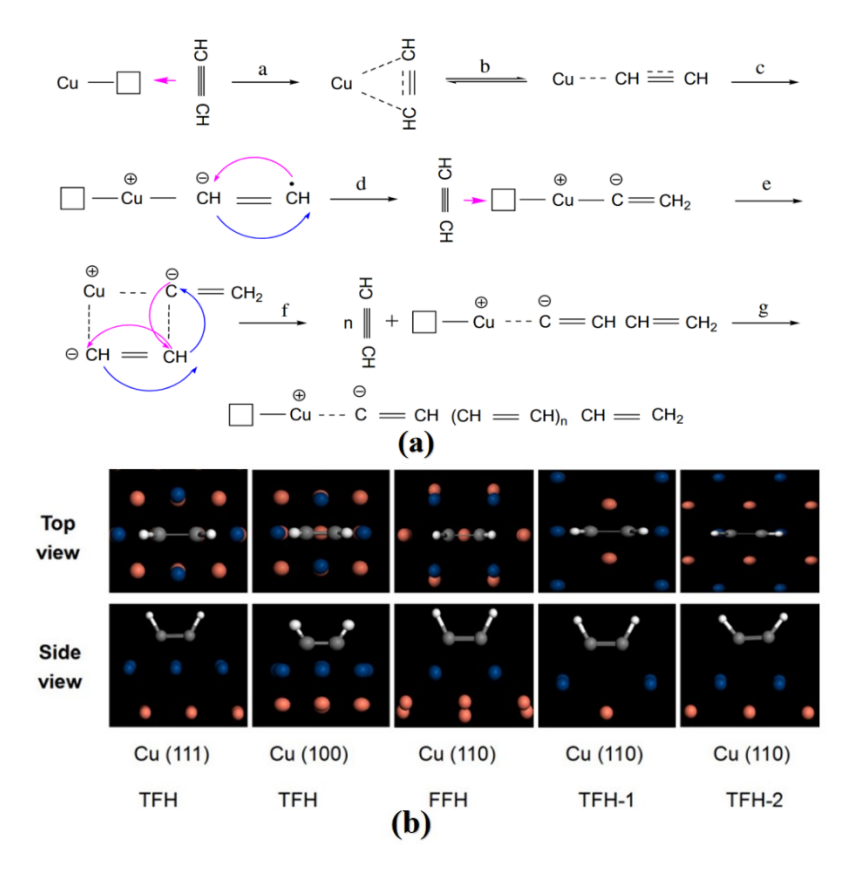


Fig. 10. (a) The diagram of the polymerization process of acetylene on copper catalyst (the small squares symbolize the unoccupied orbital of copper), (b) Optimal adsorption sites of acetylene on Cu (100), (110) and (111) surfaces. Cu atoms are denoted by large blue (the first layer) and red (internal layers) balls, C and H atoms of C₂H₂ are shown in grey and white, respectively, Copyright 2010 Elsevier Ltd. [45]

Meng et al. [46] synthesized HCNTs at 450°C using ethylene as the carbon source and α -Fe₂O₃ nanoparticles as the catalyst precursor via a trace water-assisted chemical vapor deposition method, with the growth mechanism shown in Fig. 11. Specifically, α -Fe₂O₃ is first reduced by hydrogen to form Fe, which then combines with carbon to generate Fe₃C. With Fe₃C as the catalytic core, HCNTs are efficiently synthesized with a purity close to 100%. In this growth mechanism, trace water plays a key regulatory role: on one hand, water molecules react with carbon dangling bonds to inhibit the formation of amorphous carbon; on the other hand, the addition of water enhances the anisotropy of the catalyst surface—acetylene is preferentially adsorbed on the Fe(110) crystal plane, while water is preferentially adsorbed on the Fe(111) crystal plane. This leads to differences in the precipitation rate and direction of carbon atoms on different Fe₃C crystal planes: the inner side of the graphite layer is perpendicular to the Fe₃C (020) crystal plane, while the outer side grows at a 38° angle relative to the Fe₃C (020) crystal plane, causing periodic mismatching of the graphite layers and ultimately forming HCNTs.

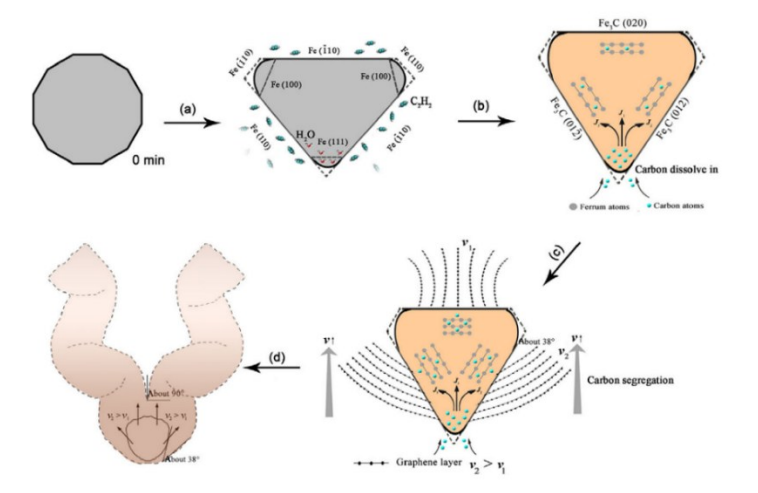


Fig. 11. Schematic of the growth process of trace-water-assisted HCNTs; (a) shape change of trace-water-induced catalyst nanoparticle, (b) process of carbon atom diffusion and segregation, (c)generation of graphite layers with helical structure, and (d) growth of HCNTs, Copyright 2018, Tsinghua University Press and Springer-Verlag GmbH Germany, part of Springer Nature [46]

The authors further verified this mechanism through DFT calculations. As shown in Fig. 12(a-b), they simulated the adsorption behaviors of C_2H_2 and H_2O on Fe (100), (110), and (111) crystal planes. It was found in the study that C_2H_2 adopts a hollow adsorption configuration on the Fe (110) crystal plane with more favorable adsorption energy, while H_2O is more stably adsorbed on the Fe (111) crystal plane. The electronic state analysis (PDOS) in Fig. 12(c-d) shows that the C atomic orbitals of C_2H_2 overlap with the 3d and 4s orbitals of Fe, and the O atomic orbitals of H_2O overlap with Fe orbitals, which respectively weaken the $C \equiv C$ bond of C_2H_2 and the O-H bond of H_2O . This confirms that the adsorption effect promotes the reaction and also provides theoretical support for the enhancement of surface anisotropy and subsequent growth differences.

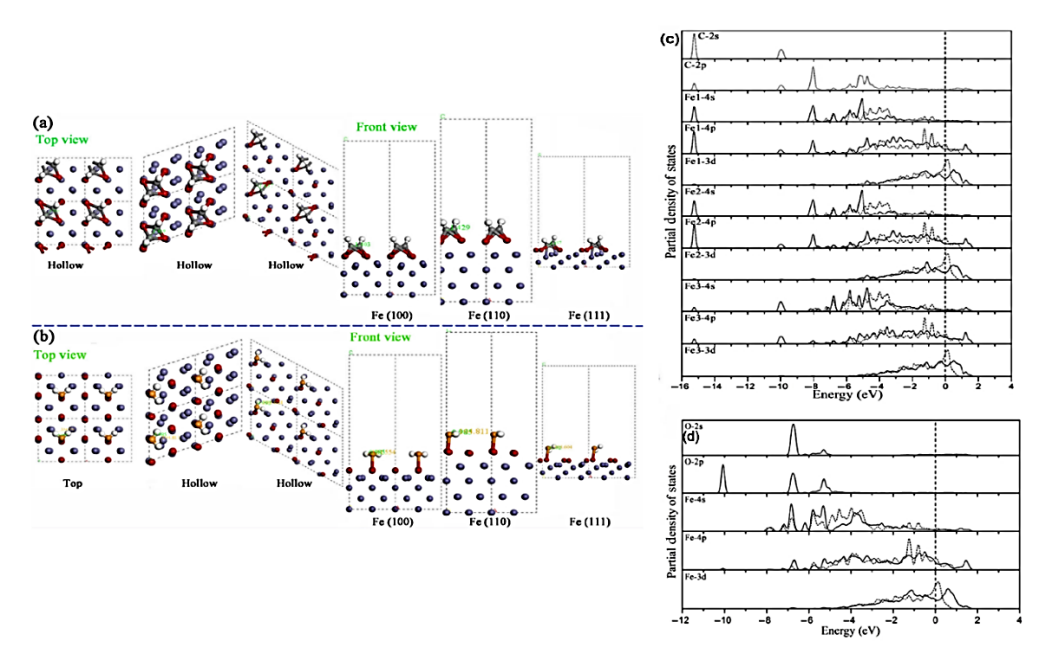


Fig. 12. Optimal adsorption sites of C₂H₂ (a) and H₂O (b) molecules on Fe (100), (110) and (111) facets, respectively. Fe atoms are denoted as red (the first layer) and purple (internal layers) spheres, and C, H, and O atoms are shown in black, white and orange spheres, respectively. The PDOS of C and Fe atoms (c) and O and Fe atoms (d). The dotted line represents "before adsorption" and the solid line represents "after adsorption", Copyright 2018, Tsinghua University Press and Springer-Verlag GmbH Germany, part of Springer Nature [46]

4. Conclusion

This paper provides a comprehensive review of the structure, preparation methods, and synthesis mechanisms of helical carbon nanofibers (HCNFs). It emphasizes that the selection of catalysts, carbon sources, and reaction conditions can effectively influence the structure of HCNFs, including their morphology. A series of catalysts, carbon sources, and different strategies can be used to synthesize HCNFs with different morphologies and coil parameters. Although certain progress has been made in the research on the preparation and mechanisms of HCNFs, there is still a need to improve the yield and uniformity of HCNFs. During the preparation process, the growth mechanisms of HCNFs with different morphologies have not been fully clarified, and clarifying the growth mechanisms is of great significance for the precise and controllable preparation of HCNFs. In addition, there is insufficient cost control and greenness level in the preparation process. In the existing preparation of HCNFs, some methods rely on noble metal catalysts or high-temperature and high-energy-consuming reaction conditions, and some carbon sources and catalyst precursors have the problem of insufficient environmental friendliness. Moreover, there is a lack of cost accounting and green optimization schemes for the entire preparation process, such as the systematic design of catalyst recovery, waste gas treatment, template recycling, and other links. This has formed a practical constraint on the transition of HCNFs from small-batch laboratory preparation to large-scale industrial application.

Acknowledgment

This work was financially supported by the National Natural Science Foundation of China (No. 52202083, W2421013), Sichuan Science and Technology Program (No. 2024YFHZ0265), and the Open Project of High-end Equipment Advanced Materials and Manufacturing Technology Laboratory (No. 2023KFKT0005).

References

- [1] W. R. Davis, R. J. Slawson, and G. R. J. N. Rigby, "An Unusual Form of Carbon," Nature, vol. 171, no. 4356, pp. 756-756, 1953,http://dx.doi.org/10.1038/171756a0.
- [2] J. F. Wen, Y. Zhang, N. J. Tang, X. G. Wan, Z. H. Xiong, W. Zhong, Z. L. Wang, X. L. Wu, and Y. W. Du, "Synthesis, Photoluminescence, and Magnetic Properties of Nitrogen-Doping Helical Carbon Nanotubes," Journal of Physical Chemistry C, vol. 115, no. 25, pp. 12329-12334, Jun 30, 2011, http://dx.doi.org/10.1021/jp202723f.
- [3] M. Z. M. Zhang, Y. N. Y. Nakayama, and L. P. L. J. J. J. o. A. P. Pan, "Synthesis of carbon tubule nanocoils in high yield using iron-coated indium tin oxide as catalyst," Japanese Journal of Applied Physics, vol. 39, no. 12A, pp. L1242, 2000,http://dx.doi.org/1347-

- 4065/39/12A/L1242.
- [4] S. Motojima, and Q. J. J. o. A. P. Chen, "Three-dimensional growth mechanism of cosmo-mimetic carbon microcoils obtained by chemical vapor deposition," Journal of Applied Physics, vol. 85, no. 7, pp. 3919-3921, 1999,http://dx.doi.org/10.1063/1.369765.
- [5] X. Chen, and S. J. C. Motojima, "The growth patterns and morphologies of carbon micro-coils produced by chemical vapor deposition," Carbon, vol. 37, no. 11, pp. 1817-1823, 1999, http://dx.doi.org/10.1016/S0008-6223(99)00054-8.
- [6] Y. Shang, Y. Li, X. He, L. Zhang, Z. Li, P. Li, E. Shi, S. Wu, and A. Cao, "Elastic carbon nanotube straight yarns embedded with helical loops," Nanoscale, vol. 5, no. 6, pp. 2403-10, Mar 21, 2013, http://dx.doi.org/10.1039/c3nr33633f.
- [7] J. C. Ruiz-Cornejo, D. Sebastián, and M. J. Lázaro, "Synthesis and applications of carbon nanofibers: a review," Reviews in Chemical Engineering, vol. 36, no. 4, pp. 493-511, May 2020, http://dx.doi.org/10.1515/revce-2018-0021.
- [8] D. Yadav, F. Amini, and A. Ehrmann, "Recent advances in carbon nanofibers and their applications A review," European Polymer Journal, vol. 138, no. 138-, pp. 138, Sep 5, 2020,http://dx.doi.org/10.1016/j.eurpolymj.2020.109963.
- [9] Shuiliang, Chen, Haoqing, Hou, Ping, Hu, Joachim, H., Wendorff, A. J. M. Materials, and Engineering, "Polymeric Nanosprings by Bicomponent Electrospinning," Macromolecular Materials and Engineering, 2009, http://dx.doi.org/10.1002/mame.200800342.
- [10] Z. Ren, and P. X. Gao, "A review of helical nanostructures: growth theories, synthesis strategies and properties," Nanoscale, vol. 6, no. 16, pp. 9366-400, Aug 21, 2014,http://dx.doi.org/10.1039/c4nr00330f.
- [11] P. E. S. Silva, F. Vistulo de Abreu, and M. H. Godinho, "Shaping helical electrospun filaments: a review," Soft Matter, vol. 13, no. 38, pp. 6678-6688, Oct 4, 2017, http://dx.doi.org/10.1039/c7sm01280b.
- [12] D. C. Wang, Y. Lei, W. Jiao, Y. F. Liu, and X. Jian, "A review of helical carbon materials structure, synthesis and applications," Rare Metals, vol. 40, no. 1, pp. 17, 2021, http://dx.doi.org/10.1007/s12598-020-01622-y.
- [13] R. Cui, D. Xu, X. Xie, Y. Yi, and G. J. F. C. Zhang, "Phosphorus-doped helical carbon nanofibers as enhanced sensing platform for electrochemical detection of carbendazim," Food Chemistry, vol. 221, pp. 457-463, 2017, http://dx.doi.org/10.1016/j.foodchem.2016.10.094.
- [14] Xinglong, Zheng, Yongzhong, Jin, Jian, Chen, Binghong, Li, Qingshan, and F. J. J. o. M. Science, "Mechanical properties and microstructure characterization of natural rubber reinforced by helical carbon nanofibers," Journal of Materials Science, vol. 54, no. 19, pp. 12962–12971, 2019,http://dx.doi.org/10.1007/s10853-019-03771-7.
- [15] X. Guo, X. Li, L. Xia, L. Ma, W. Lü, and K. J. A. A. N. M. Li, "Controllable Preparation of Helical Carbon Nanofibers for Electromagnetic Wave Absorption," ACS Applied Nano Materials, vol. 7, no. 17, pp. 10, 2024, http://dx.doi.org/10.1021/acsanm.4c03454.
- [16] D. Jiang, Y. Jin, W. Zhang, X. Li, G. Chen, and Y. J. J. o. E. C. Liu, "Helical carbon nanofibers-supported MnSiO3 for high-performance lithium-ion battery anode materials," Electrochimica Acta, pp. 977, 2025, http://dx.doi.org/10.1016/j.electacta.2025.146844.
- [17] X. X. Zhou, Y. Wang, C. C. Gong, B. Liu, and G. Wei, "Production, structural design, functional control, and broad applications of carbon nanofiber-based nanomaterials: A comprehensive review," Chemical Engineering Journal, vol. 402, pp. 126189, Dec 15, 2020,http://dx.doi.org/10.1016/j.cej.2020.126189.
- [18] Y. Qin, Z. Zhang, and Z. J. C. Cui, "Helical carbon nanofibers with a symmetric growth mode," Carbon, vol. 42, no. 10, pp. 1917-1922, 2004,http://dx.doi.org/10.1016/j.carbon.2004.03.020.
- [19] N. Tang, W. Zhong, A. Gedanken, and Y. Du, "High magnetization helical carbon nanofibers produced by nanoparticle catalysis," J Phys Chem B, vol. 110, no. 24, pp. 11772-4, Jun 22, 2006, http://dx.doi.org/10.1021/jp060004b.
- [20] L. Yu, Y. Qin, and Z. J. M. L. Cui, "Synthesis of coiled carbon nanofibers by Cu–Ni alloy nanoparticles catalyzed decomposition of acetylene at the low temperature of 241° C," Materials Letters, vol. 59, no. 4, pp. 459-462, 2005,http://dx.doi.org/10.1016/j.matlet.2004.10.021.
- [21] J. L. Fajardo-Díaz, S. M. Durón-Torres, F. López-Urías, and E. Muñoz-Sandoval, "Synthesis, characterization and cyclic voltammetry studies of helical carbon nanostructures produced by thermal decomposition of ethanol on Cu-foils," Carbon, vol. 155, pp. 469-482, Dec, 2019,http://dx.doi.org/10.1016/j.carbon.2019.09.015.
- [22] R. Cui, Z. Han, and J. J. Zhu, "Helical carbon nanotubes: intrinsic peroxidase catalytic activity and its application for biocatalysis and biosensing," Chemistry, vol. 17, no. 34, pp. 9377-84, Aug 16, 2011,http://dx.doi.org/10.1002/chem.201100478.
- [23] I. J. D. Priscillal, S. F. Wang, and S. Kameoka, "Investigation on the influence of reaction temperature on the structural and magnetic properties of morphologically diverse carbon nanotubes synthesized using LaNi5Pt0.5 alloy catalyst," Journal of Alloys and Compounds, vol. 958, pp. 170355, Oct 5, 2023, http://dx.doi.org/10.1016/j.jallcom.2023.170355.
- [24] H. Radnia, A. Rashidi, and A. R. S. Nazar, "Synthesis of Helical and Straight Carbon Nanofibers on Water Soluble Sodium Chloride Supported Catalyst," Journal of Inorganic and Organometallic Polymers and Materials, vol. 30, no. 5, pp. 1600-1608, May, 2020,http://dx.doi.org/10.1007/s10904-019-01381-z.
- [25] Y. Z. Jin, J. Chen, Q. S. Fu, B. H. Li, H. Z. Zhang, and Y. Gong, "Low-temperature synthesis and characterization of helical carbon fibers by one-step chemical vapour deposition," Applied Surface Science, vol. 324, pp. 438-442, Jan 1, 2015,http://dx.doi.org/10.1016/j.apsusc.2014.10.107.
- [26] X. Jian, M. Jiang, Z. W. Zhou, Q. Zeng, J. Lu, D. C. Wang, J. T. Zhu, J. H. Gou, Y. Wang, D. Hui, and M. L. Yang, "Gas-Induced Formation of Cu Nanoparticle as Catalyst for High-Purity Straight and Helical Carbon Nanofibers," Acs Nano, vol. 6, no. 10, pp. 8611-8619, Oct, 2012, http://dx.doi.org/10.1021/nn301880w.
- [27] Y. Suda, K. Maruyama, T. Iida, H. Takikawa, H. Ue, K. Shimizu, and Y. Umeda, "High-Yield Synthesis of Helical Carbon Nanofibers Using Iron Oxide Fine Powder as a Catalyst," Crystals, vol. 5, no. 1, pp. 47-60, Mar, 2015, http://dx.doi.org/10.3390/cryst5010047.
- [28] Y. Li, S. Guo, L. Zhao, S. Chen, Y. Li, X. Yang, P. Wang, W. Feng, Z. Mou, and H. J. C. Jiang, "Controlled preparation of lightweight, resilient helical carbon fibers for high-performance microwave absorption and oil-water separation," Carbon, vol. 233, pp. 119923, 2025, http://dx.doi.org/10.1016/j.carbon.2024.119923.
- [29] X. Xiong, P. Zhao, R. Ren, X. Cui, and S. Ji, "Flame-Synthesis of Carbon Nanotube Forests on Metal Mesh Structure: Dependence, Morphology, and Application," Nanomaterials (Basel), vol. 9, no. 9, pp. 1188, Aug 22, 2019, http://dx.doi.org/10.3390/nano9091188.
- [30] W. Zhang, Q. S. Fu, X. D. Chen, Z. X. Yu, Y. Z. Jin, N. Q. Liu, Y. P. Sheng, L. L. Xiao, and J. Chen, "Facile yet versatile assembling of helical carbon nanofibers via metal-organic frameworks burned in ethanol flame and their electrochemical properties as electrode of supercapacitor," Journal of Power Sources, vol. 521, pp. 230908, Feb 15, 2022, http://dx.doi.org/10.1016/j.jpowsour.2021.230908.
- [31] L. Thirugnanam, M. Palanisamy, S. Kaveri, S. Ramaprabhu, V. G. Pol, and M. Dutta, "TiO nanoparticle embedded nitrogen doped electrospun helical carbon nanofiber-carbon nanotube hybrid anode for lithium-ion batteries," International Journal of Hydrogen Energy,

- vol. 46, no. 2, pp. 2464-2478, Jan 6, 2021, http://dx.doi.org/10.1016/j.ijhydene.2020.10.149.
- [32] X. Zha, Y. Chen, H. Fan, Y. Yang, Y. Xiong, G. Xu, K. Yan, Y. Wang, Y. Xie, and D. J. A. C. I. E. Wang, "Handedness Inversion of Chiral 3-Aminophenol Formaldehyde Resin Nanotubes Mediated by Metal Coordination," Angewandte Chemie, vol. 60, no. 14, pp. 7759-7769, 2021, http://dx.doi.org/10.1002/ange.202013790.
- [33] Z. L. Xiao, Y. M. Guo, B. Z. Li, and Y. Li, "Preparation and Characterization of Single-handed Helical Carbonaceous Nanofibers using 1,4-Phenylene Bridged Polybissilsesquioxanes," Journal of Wuhan University of Technology-Materials Science Edition, vol. 31, no. 5, pp. 1149-1154, Oct, 2016,http://dx.doi.org/10.1007/s11595-016-1504-7.
- [34] E. J. Cho, L. T. P. Trinh, Y. Song, Y. G. Lee, and H. J. Bae, "Bioconversion of biomass waste into high value chemicals," Bioresource Technology, vol. 298, pp. 122386, Feb, 2020,http://dx.doi.org/10.1016/j.biortech.2019.122386.
- [35] W. Wang, A. Saeed, J. He, Z. Wang, D. Zhan, Z. Li, C. Wang, Y. Sun, F. Tao, and W. Xu, "Bio-inspired porous helical carbon fibers with ultrahigh specific surface area for super-efficient removal of sulfamethoxazole from water," J Colloid Interface Sci, vol. 578, pp. 304-314, Oct 15, 2020, http://dx.doi.org/10.1016/j.jcis.2020.05.117.
- [36] J. Gavillet, A. Loiseau, C. Journet, F. Willaime, F. Ducastelle, and J. C. Charlier, "Root-growth mechanism for single-wall carbon nanotubes," Phys Rev Lett, vol. 87, no. 27 Pt 1, pp. 275504, Dec 31, 2001, http://dx.doi.org/10.1103/PhysRevLett.87.275504.
- [37] M. Kawaguchi, K. Nozaki, S. Motojima, and H. J. J. o. C. G. Iwanaga, "A growth mechanism of regularly coiled carbon fibers through acetylene pyrolysis," Journal of Crystal Growth, vol. 118, no. 3-4, pp. 309-313, 1992,http://dx.doi.org/10.1016/0022-0248(92)90077-v.
- [38] R. S. Wagner, and W. C. J. A. p. l. Ellis, "Vapor-liquid-solid mechanism of single crystal growth," Applied Physics Letters, vol. 4, no. 5, pp. 89-90, 1964,http://dx.doi.org/10.1063/1.1753975.
- [39] X. Chen, T. Saito, M. Kusunoki, and S. J. J. o. m. r. Motojima, "Three-dimensional vapor growth mechanism of carbon microcoils," Journal of Materials Research, vol. 14, no. 11, pp. 4329-4336, 1999,http://dx.doi.org/10.1557/JMR.1999.0586.
- [40] X. Chen, S. Yang, and S. J. M. l. Motojima, "Morphology and growth models of circular and flat carbon coils obtained by the catalytic pyrolysis of acetylene," Materials Letters, vol. 57, no. 1, pp. 48-54, 2002, http://dx.doi.org/10.1016/s0167-577x(02)00697-3.
- [41] S. Motojima, X. Chen, S. Yang, M. J. D. Hasegawa, and R. Materials, "Properties and potential applications of carbon microcoils/nanocoils," Diamond and Related Materials, vol. 13, no. 11-12, pp. 1989-1992, 2004,http://dx.doi.org/10.1016/j.diamond.2004.06.020.
- [42] W. J. Li, H. T. Xu, Y. C. Guo, and L. J. J. A. P.-C. S. Chen, "Vapor-Liquid-Solid-Solid Growth Mechanism of Carbon Micro-coils," Acta Physico-Chimica Sinica, 2006, http://dx.doi.org/10.3866/PKU.WHXB20060625.
- [43] A. Shaikjee, and N. J. Coville, "The role of the hydrocarbon source on the growth of carbon materials," Carbon, vol. 50, no. 10, pp. 3376-3398, Aug, 2012,http://dx.doi.org/10.1016/j.carbon.2012.03.024.
- [44] F. Nitze, E. Abou-Hamad, and T. Wågberg, "Carbon nanotubes and helical carbon nanofibers grown by chemical vapour deposition on C fullerene supported Pd nanoparticles," Carbon, vol. 49, no. 4, pp. 1101-1107, Apr, 2011,http://dx.doi.org/10.1016/j.carbon.2010.11.015.
- [45] X. A. Jian, M. Jiang, Z. W. Zhou, M. L. Yang, J. Lu, S. C. Hu, Y. Wang, and D. Hui, "Preparation of high purity helical carbon nanofibers by the catalytic decomposition of acetylene and their growth mechanism," Carbon, vol. 48, no. 15, pp. 4535-4541, Dec, 2010, http://dx.doi.org/10.1016/j.carbon.2010.08.035.
- [46] F. B. Meng, Y. Wang, Q. Wang, X. L. Xu, M. Jiang, X. S. Zhou, P. He, and Z. W. Zhou, "High-purity helical carbon nanotubes by trace-water-assisted chemical vapor deposition: Large-scale synthesis and growth mechanism," Nano Research, vol. 11, no. 6, pp. 3327-3339, Jun, 2018, http://dx.doi.org/10.1007/s12274-017-1897-4.